



POLİTEKNİK DERGİSİ

*JOURNAL of POLYTECHNIC*

ISSN: 1302-0900 (PRINT), ISSN: 2147-9429 (ONLINE)

URL: <http://dergipark.org.tr/politeknik>



# Investigation mechanical and microstructural behavior of operated and unoperated turbine rotor discs

## *Kullanılmış ve kullanılmamış türbin rotor disklerinin mekanik ve mikroyapısal davranışlarının incelenmesi*

*Yazar(lar) (Author(s)):* Elif UZUN KART<sup>1</sup>, Cemre ÖZGÜL<sup>2</sup>

*ORCID<sup>1</sup>:* 0000-0002-4950-2162

*ORCID<sup>2</sup>:* 0000-0003-3071-3717

**To cite to this article:** Uzun Kart E. ve Özgül C., “Investigation mechanical and microstructural behavior of operated and unoperated turbine rotor discs”, *Journal of Polytechnic*, 26(2): 743-749, (2023).

**Bu makaleye şu şekilde atıfta bulunabilirsiniz:** Uzun Kart E. ve Özgül C., “Investigation mechanical and microstructural behavior of operated and unoperated turbine rotor discs”, *Politeknik Dergisi*, 26(2): 743-749, (2023).

**Erişim linki (To link to this article):** <http://dergipark.org.tr/politeknik/archive>

**DOI:** 10.2339/politeknik.1062820

# Investigation Mechanical and Microstructural Behavior of Operated and Unoperated Turbine Rotor Discs

## Highlights

- ❖ In gas turbine engines, turbines are exposed to higher temperatures and loads during operation.
- ❖ The effects of the service conditions on the microstructure of both rotors were primary and secondary carbides in the gamma matrix that had Cr and W were deposited at grain boundaries as  $M_{23}C_6$  secondary carbides.
- ❖ Hf, Ta, and Ti elements precipitated as MC carbides causing increased gamma prime volume and solid solution hardening of super-alloy Mar M-247.

## Graphical Abstract

In this study, Mar M-247 polycrystalline cast turbine rotor operated at Turbojet Engine, which was developed in Kale R&D Inc., and the unoperated turbine rotor that was produced from the same material were examined about its mechanical and microstructural properties.

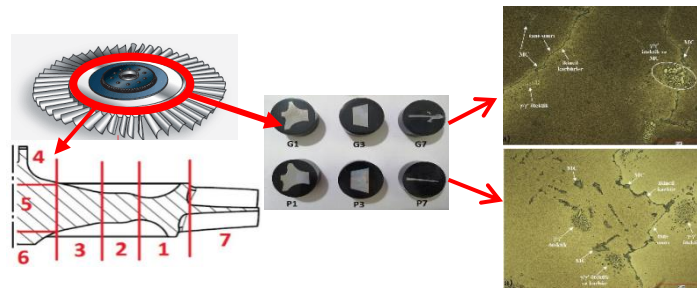


**Figure A.** The operated and unoperated jet rotor sampling and representative microstructures.

## Aim

Polycrystalline Ni-based super-alloy Mar M-247 turbines that had the same design and that were produced to be used in turbojet engines after undergoing two step aging heat-treatment were examined in the aim of this study.

## Design & Methodology

Operated and non-operated turbine rotor discs were cut by wire erosion, and 6 samples extracted from the disc region of the turbines were tested to high-temperature tensile test, hardness and microstructure analysis.

## Originality

In gas turbine engines, turbines are exposed to higher temperatures and loads during operation however, operated and non-operated in turbojet engines were compared with their physical properties.

## Findings

Blocky and Chinese script-like carbides and gamma prime eutectic islands were found in both turbine structures and tensile strength, ductility, and hardness of the operated turbine increased.

## Conclusion

Service conditions had no significant impacts on the microstructure of the non-operated rotor disc but the difference in  $\gamma'$  volume/fraction supports the idea that the operated rotor disc continues to age during service life.

## Declaration of Ethical Standards

The author(s) of this article declare that the materials and methods used in this study do not require ethical committee permission and/or legal-special permission.

# Investigation Mechanical and Microstructural Behavior of Operated and Unoperated Turbine Rotor Discs

## Research Article

Elif UZUN KART<sup>1\*</sup>, Cemre ÖZGÜL<sup>2</sup>

<sup>1</sup> Teknoloji Fakültesi, Metalurji ve Malzeme Mühendisliği Bölümü, Marmara Üniversitesi, Türkiye

<sup>2</sup> Fen Bilimleri Enstitüsü, Metalurji ve Malzeme Mühendisliği ABD, Marmara Üniversitesi, Türkiye

(Geliş/Received : 25.01.2022 ; Kabul/Accepted : 02.02.2022 ; Erken Görünüm/Early View : 21.02.2022)

## ABSTRACT

In gas turbine engines, turbine sections are exposed to high temperature and loads during operation and therefore turbine inlet boundary is considered the most challenging for turbomachines. Ni-based super-alloys are used for turbine materials in gas turbine engines because of their superior mechanical characteristics at high temperatures. In this research, two Mar M-247 polycrystalline cast Ni-based turbine rotors, which were operated and non-operated in turbojet engine tests, had the same design and applied the same two-step aging heat treatment, were examined microstructurally and mechanically. As a result of the mechanical analysis, it was observed that the tensile strength (Rm (P): 537Mpa; Rm (G): 590 Mpa) ductility, and hardness (429 HV (P), 440 HV (G)) of the operated turbine rotor increased. In the microstructure analysis, blocky and Chinese script-like carbides and gamma prime eutectic islands were found in both turbine structures. EDS analysis showed that the carbides in the matrix are rich in Hf, Ta, and Ti, and the grain boundary carbides are rich in Cr and W.

**Keywords:** Mar M-247, Ni-based super-alloys, gas turbine turbojet engines

## 1. INTRODUCTION

Ni-based super-alloys are used commonly in challenging conditions like gas turbine engines with their high strength, long fatigue life, fracture toughness, and high corrosion resistance at high temperatures [1], [2], [3], [4], [5], [6]. Ni-based super-alloy Mar M-247 exhibits excellent resistance to high temperatures, to high thermomechanical loads along with superior creep and fatigue behaviors, hot corrosion resistance, and good castability characteristics [7], [8], [9], [10]. Mar M-247

Mar M-247 super-alloy, which has a face-centered cubical-crystal structure, is hardened by solid-solution hardening of Ta, W, and Mo, and the  $\gamma'$  particles that have a volume fraction at 60% precipitated in the  $\gamma$  matrix [7], [9], [14]. When the cage wrong matches between the  $\gamma'$  phase and the matrix phase is below 1%, the alloy can remain stable for longer durations at high temperatures [14], [15].

Precipitation hardening heat treatment is applied to some cast super-alloys that are employed at high temperatures to increase the hardness and strength [14], [16]. The distribution and morphology of the carbides in the matrix are improved with heat treatment, and mechanical characteristics of the alloy can be improved in this way [7], [17]. Secondary carbides deposited on the grain boundaries stabilize the grain boundaries against shear by preventing the movement of dislocations and improve the plasticity, creep and stress-rupture strength of the alloy [16], [18]. Primary carbides precipitate in different morphologies, e.g. blocky particles and Chinese script, and secondary carbides, e.g. blocky particles, plates, and Widmanstätten [2], [16]. Primary carbides, which

Ni-based super-alloy was developed at Martin Metals Corporation in the 1970s, is used widely in aircraft engines and in the production of components that are subjected to higher temperatures and stress, such as turbine blades with its superior characteristics [7], [8], [9], [10], [11], [12]. Mar M-247 is a cast super-alloy that has a volume fraction of  $\gamma'$  Ni<sub>3</sub>(Al, Ti) and a high-rate refractory element contents such as Ta, W, and Mo (14% by weight) [9], [10], [11], [12], [13]. Its chemical composition is given in Table 1 [14].

precipitate in Chinese script-like morphology, are considered detrimental as they cause crack initiation and propagation [16].

Polycrystalline Ni-based super-alloy Mar M-247 turbines that had the same design and that were produced to be used in turbojet engines after undergoing two step aging heat-treatment were examined in the aim of this study. During the operation of the turbojet engine, the effects of the compelling service conditions of Mar M-247 super-alloy turbine on the micro-structure and mechanical characteristics of the alloy, phase structure, strength, hardness, and elongation of the alloy were examined, and the results were correlated with service conditions.

## 2. MATERIALS and METHOD

In this research, two Mar M-247 polycrystalline cast Ni-based turbines, which were operated and non-operated in turbojet engine tests, had the same design and applied the same two-step aging heat treatment, were examined microstructurally and mechanically. The elemental composition of these turbines is given in Table 2. Both turbines were applied to two-step aging heat treatments after casting. One of the turbines was operated in turbojet

\*Sorumlu Yazar (Corresponding Author)  
e-posta : elif.uzun@marmara.edu.tr

engine tests, and was coded with “G”, and the unoperated turbine was coded “P”. The G turbine operated on the turbojet engine for approximately 16 minutes. It was determined in the thermal analysis that the turbine rotor

blade area was exposed to an optimum temperature of 1000°C and the turbine rotor disc area to 500-600°C under maximum service conditions of the turbojet engine.

**Table 1.** Mar M-247 nominal chemical composition [14].

Element	C	Cr	Co	W	Mo	Ta	Al	Ti	Hf	B	Zr	Ni
Percentage	0.15	8.3	10.0	10.0	0.7	3.0	5.5	1.0	1.5	0.015	0.05	Balance

**Table 1.** Elemental compositions of P and G turbine rotors.

Element	C	Cr	Co	W	Mo	Ta	Al	Ti	Hf	B	Zr	Ni
P	0.154	8.22	9.14	9.96	0.650	3.22	5.55	1.05	1.53	0.0146	0.0307	60.2
G	0.136	8.36	9.34	9.88	0.736	3.12	5.65	1.06	1.24	0.0125	0.0327	60.0

P and G turbines were cut by wire erosion, and 3 samples extracted from the disc region of the turbines were tested to high-temperature tensile test, which was performed with Zwick Roell Z600 Device at 980°C. Also, a cross-sectional slice was taken from the center of the turbine discs to the outer diameter, which was then cut into pieces with wire erosion for microhardness measurements and metallographic examinations (Figure 1). Samples 1, 3, and 7 were prepared for metallographic examinations. The samples were examined under the optical microscope before and after etching, and the SEM-EDS examination was performed afterward.

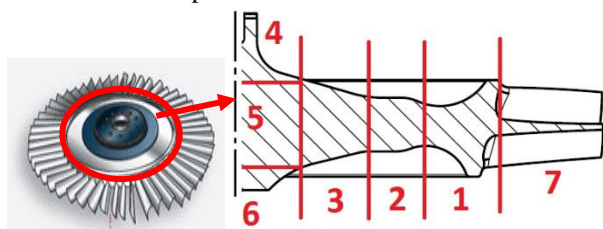


**Figure 1.** Section geometry of turbojet turbine disc.

### 3. RESULTS and DISCUSSION

#### 3.1. Hardness Test

The microhardness results of the samples taken from P and G turbine rotor discs are given in Table 3. According to microhardness measurement results, the hardness of G turbine disc that was taken from the operated turbine rotor was found to be higher than that of P turbine disc that was taken from the unoperated turbine rotor. It was reported in the literature that the hardness and material strength increase with precipitation hardening [14], [19]. It was considered that the operated turbine rotor continues to age during service and its hardness increases due to aging.

#### 3.2. High-Temperature Tensile Test

The samples that were taken from P and G turbine discs were tested to high-temperature tensile test at 980°C, and the results are given in Table 4.

According to the results of high-temperature tensile test, it was found that the tensile strength of G turbine discs

was higher than that of P turbine discs; and although no significant differences were detected between the yield strengths, the yield strength of G turbine discs was also approximately equal. Based on the finding that the tensile strength and hardness of G turbine discs were higher than P turbine discs, the idea that the operated turbine rotor continued to age during service was supported. According to the test results, it was detected that the G turbine discs were elongated more than the P turbine discs, and its ductility increased. Martinsson was found that the yield strength, tensile strength, and hardness of Haynes 230 Ni-based super-alloy samples increased and became more ductile by aging [20].

**Table 2.** Micro hardness results.

Sample	HV
P	429
G	440

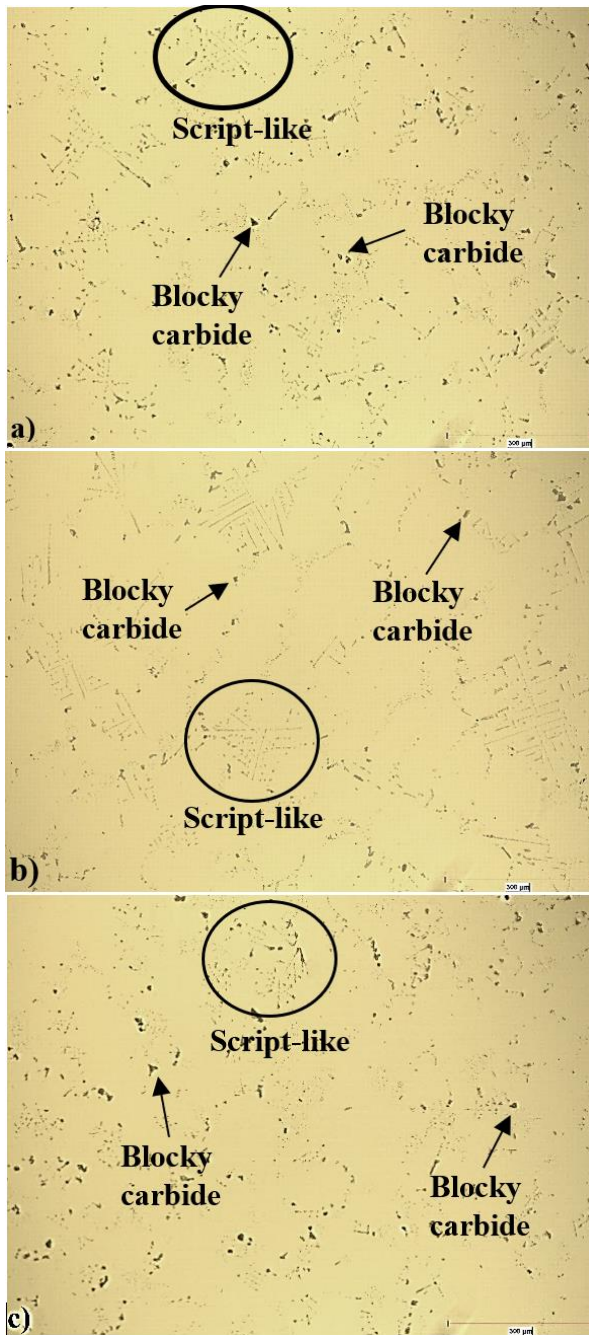
**Table 4.** High-temperature tensile test results.

Turbine	Temperature (°C)	R <sub>p0.2</sub> (MPa)	R <sub>m</sub> (MPa)	A (%)
P	980	427	537	2,1
G	980	433	590	3,5

#### 3.3. Metallography Images and Analysis

The microstructure images of unetched P turbine discs are shown in Figure 2. As a result of the examination of the unetched P and G turbine discs under an optical microscope, primary and secondary carbides were detected in the  $\gamma$  matrix with different morphologies such as Chinese script and blocky. The carbides were positioned in the interdendritic areas. It was found in the samples that were taken from the rotors that the dominant unetched G turbine discs and the surface image was 10 times zoomed to illustrate the microstructure in Figure 3. Carbide morphology in the matrix was Chinese script-like primary MC carbides. The microstructure images of

In the microstructure of the etched P and G turbines, large  $\gamma/\gamma'$  eutectic islands were detected at and near the grain boundaries in the  $\gamma$  matrix. Also, MC primary carbides that were dispersed in the matrix and primary and



secondary carbides precipitated at grain boundaries. There were carbide deposits in and around  $\gamma/\gamma'$  eutectic islands.

**Figure 2.** Microstructure of unetched P turbine discs, a) P1, b) P3, c) P7.

The microstructure images of etched P turbine discs that the surface image was 50 times zoomed to illustrate the microstructure in Figure 4.

The microstructure images of the etched G turbine discs that the surface image was 50 times zoomed to illustrate the microstructure in Figure 5.

Wawro investigated air-cooled cast Mar M-247 turbine blades heat treated at 870 °C for 16 hours. It was reported that MC carbides were found in interdendritic areas and formed script-like structures. He also said that the script-

like structures had grain boundaries and arms that extended to  $\gamma'$  islands, and that, small amounts of  $M_{23}C_6$  carbides were detected at the grain-boundaries and around the  $\gamma'$  islands.  $M_{23}C_6$  carbides were in the form of discrete, blocky, and spherical particles [21].

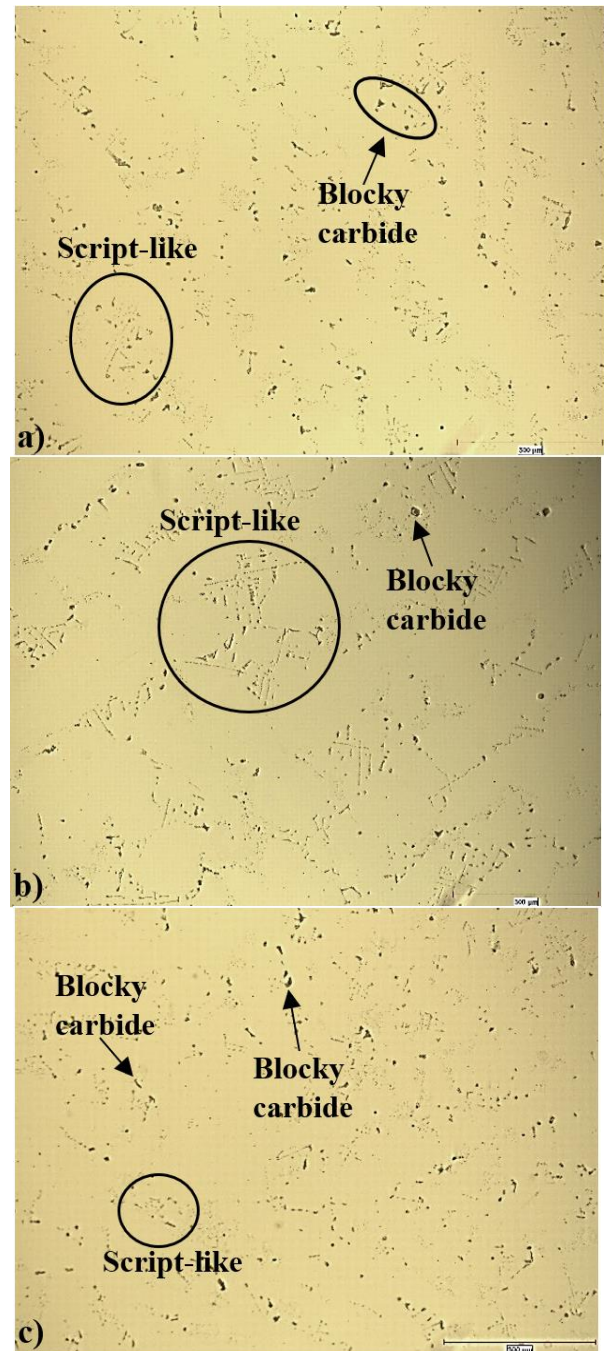


**Figure 3.** Microstructure of unetched G turbine discs, a) G1, b) G3, c) G7.

Szczotok and Rodak, in their study examining the microstructure of the Mar M-247 super-alloy, reported that carbides were found at the grain-boundaries and interdendritic areas. Numerous MC carbides were also detected in and around the  $\gamma/\gamma'$  eutectic, and carbides (MC) were in the form of clusters, and discrete blocky precipitates at various shapes and sizes. The predominant

morphology of these carbides, which can be seen at low magnifications (up to ca. 1500X), was reported to be

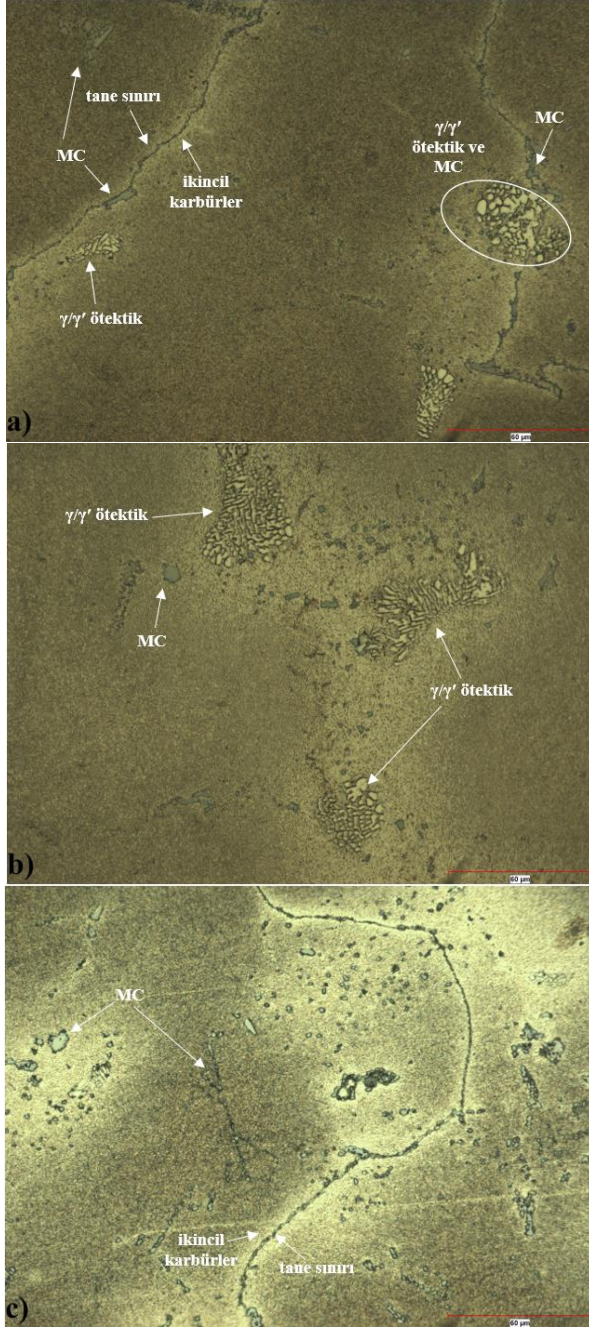


**Figure 4.** Micro-structure of etched P turbine discs a) P1, b) P3, c) P7.

“Chinese script-like” precipitates in interdendritic areas. It was also found that  $M_{23}C_6$  carbides were at the grain-boundaries and edges of  $\gamma'$  islands [18]. It was seen with optical microscope examination that there were carbides of different morphologies in the microstructure of the samples that were taken from both rotors. Carbides, which were reported to increase grain boundary strength by preventing grain boundaries from slipping, were detected in the microstructure [2], [16], [18].

### 3.4. SEM-EDS Analysis

As a result of the optical microscope examination of the samples that were taken from Mar M-247 polycrystalline

cast turbine rotor discs, carbides (primary/ secondary) in the microstructure were examined under SEM; and then, the EDS analysis of the carbides was performed. Primary and secondary carbides dispersed in  $\gamma$  matrix and deposited at grain boundaries in the microstructure are shown in Figure 6 and 7.

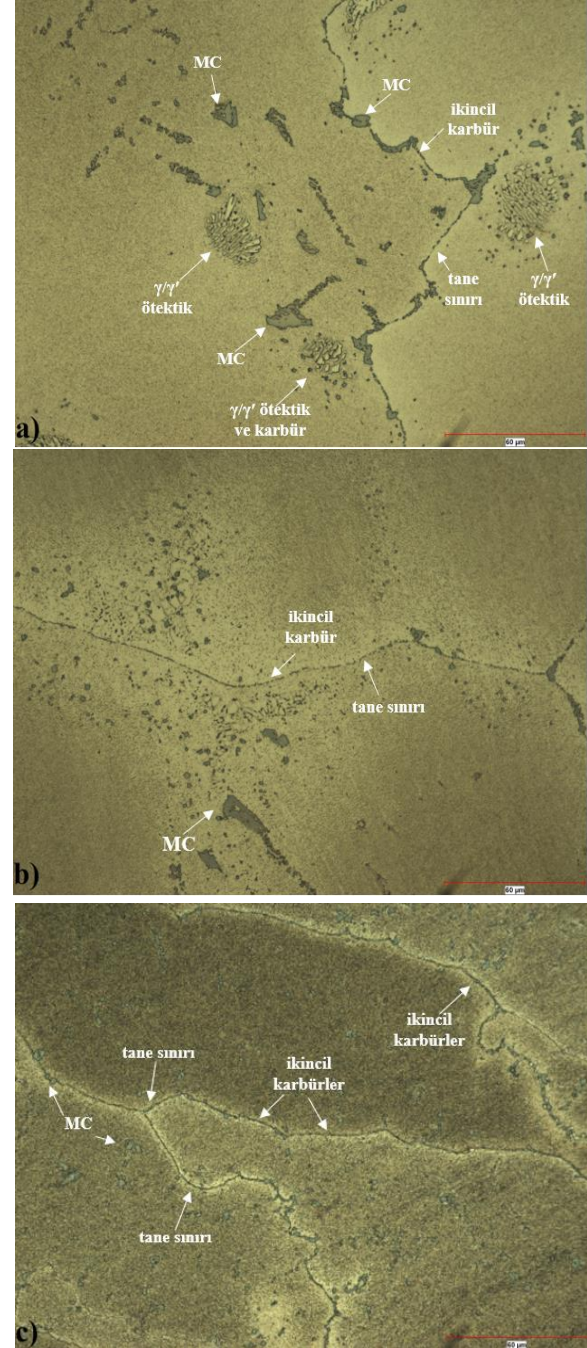


**Figure 5.** Microstructure of etched G turbine discs, a) G1, b) G3, c) G7.

The EDS analysis was performed on the carbides in the grain boundaries of the samples that were taken from the P and G turbine discs. As a result of this analysis, it was found that the grain boundary carbides had high Cr and W contents (Fig. 8). The carbides that had Cr and W were deposited at grain boundaries as secondary carbides. It is already known that secondary carbides in the grain

boundaries increase the strength and creep resistance of the super-alloy [16], [18], [22].

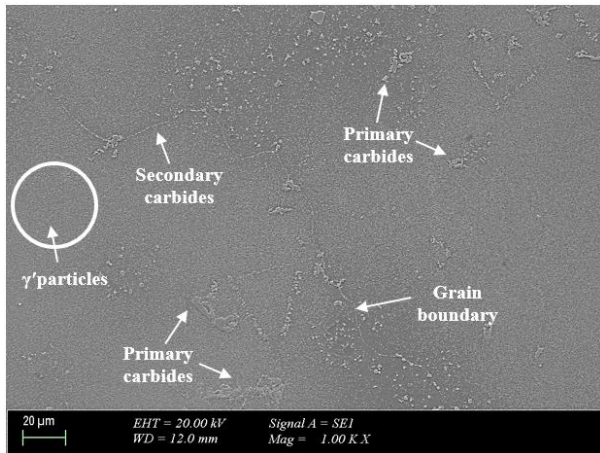


Figure 6. SEM image of P turbine disc.

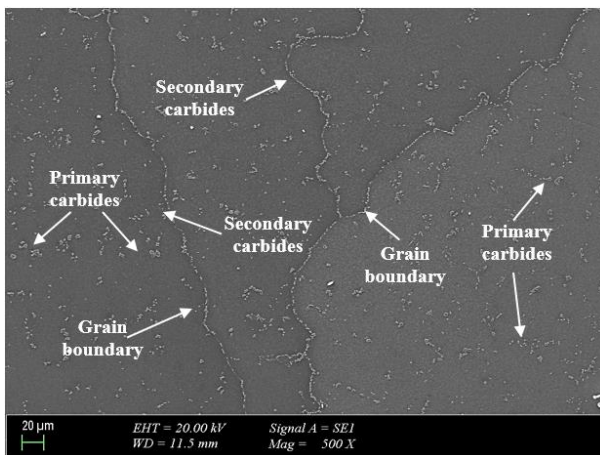


Figure 7. SEM image of G turbine disc.

It was found as a result of the EDS analysis that the primary carbides had high-content Hf and Ta, and lesser Ti amounts (Figure 9 and 10). It was reported in the literature that carbides that had Hf, Ta, and Ti in their structures dispersed in the  $\gamma$  matrix yielded solid solution hardening and increased  $\gamma'$  volume fraction [16], [19], [23], [24]. It was also reported that Hf changed the MC carbide structure from a script morphology to a blocky morphology; and that adding hafnium also caused the formation of larger  $\gamma'$  islands amounts mainly at the grain boundaries [21].

The  $\gamma'$  volume fraction of the samples that were taken from both rotors were measured, and it was found that the  $\gamma'$  volume fraction of the sample that was taken from the P rotor was ca. 74.7% and the  $\gamma'$  volume fraction of the sample that was taken from the G turbine disc was ca. 76.7%. It was reported in the literature that the strength increased up to a certain point with increased  $\gamma'$  volume fraction [14], [25-27]. The fact that the  $\gamma'$  volume fraction and strength of the G turbine disc were higher than the P rotor indicates that it is consistent with the literature.

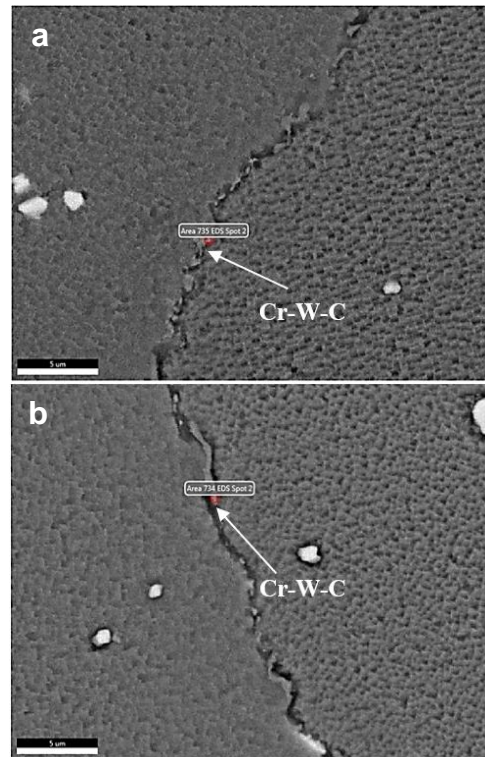


Figure 8. SEM images of P (left) and G (right) turbine discs grain boundaries.

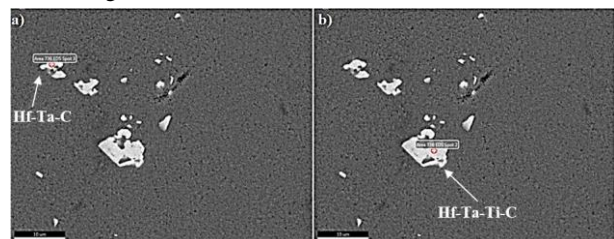


Figure 9. SEM image of P turbine disc's carbides.

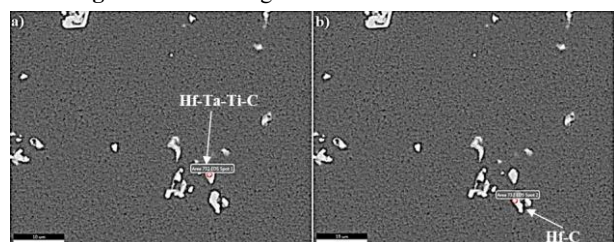


Figure 10. SEM image of G turbine disc's carbides.

#### 4. CONCLUSION

In the scope of this study, the Mar M-247 polycrystalline cast turbine rotor operated at Turbojet Engine, which was developed in Kale R&D Inc., and the unoperated turbine rotor that was produced from the same material were examined. The effects of the service conditions on the microstructure and mechanical characteristics of the material were also investigated in this respect. The conclusions that were reached in the light of the examinations are given below.

- According to Vickers Microhardness Measurement results, the hardness of the sample that was taken from the operated turbine rotor disc was found to be higher than that of the sample that was taken from the unoperated turbine rotor disc. The fact that the operated turbine rotor was harder suggests that it continues to age during its service period.
- It was observed according to the results of the high-temperature tensile test on the samples of both rotors that the tensile strength of the operated turbine rotor was higher than that of the unoperated turbine rotor. The higher tensile strength and hardness of the operated rotor support the idea that aging continues during service life. Also, the amount of elongation of the operated turbine rotor increased with aging, and became more ductile.
- It was observed as a result of the metallographic examination of the samples that were taken from both rotor discs that there were carbides (primary/secondary) in the gamma matrix that had different morphologies such as Chinese script and blocky. The carbides are found in the interdendritic areas. It was determined in the samples that were taken from both rotors that the dominant carbide morphology was Chinese script-like primary MC carbides in the matrix. It was observed in the microstructure of the etched samples that there were large  $\gamma/\gamma'$  eutectic islands at and near the grain boundaries in the gamma matrix. It was also found that there were MC primary carbides diffused in the matrix and primary and secondary carbides precipitated at grain boundaries. Carbide deposits were also found in and around  $\gamma/\gamma'$  eutectic islands.
- As a result of the EDS analysis on the carbides in the grain boundaries of the samples that were taken from both rotors, it was observed that the grain boundary carbides had high Cr and W contents. The carbides that had Cr and W were deposited at grain boundaries as M23C6 secondary carbides. Also, it was found as a result of the EDS analysis of the carbides in the  $\gamma$  matrix that the primary carbides had high-levels Hf, Ta, and less Ti. M23C6 secondary carbides deposited on the grain boundaries increased grain boundary strength. Hf, Ta, and Ti elements precipitated as MC carbides causing increased gamma prime volume and solid solution hardening of super-alloy Mar M-247.
- Service conditions had no significant impacts on the microstructure of the material. According to the gamma prime volume/fraction measurements, the  $\gamma'$  volume fraction of the sample that was taken from the P rotor disc was ca. 74.7% and the  $\gamma'$  volume/fraction of the sample that was taken from the G rotor was ca. 76.7%. The difference in  $\gamma'$  volume/fraction supports the idea that the G rotor disc continues to age during service life.

#### ACKNOWLEDGEMENT

The present study was supported by Kale Arge Inc. and Marmara University Scientific Research Projects Coordination Unit (FEN-C-YLP-100719-0244). We would like to thank these institutions for their support.

#### SYMBOLS AND ABBREVIATIONS

Mar M-247: Nickel based superalloy  
 Ni-Based: Nickel based  
 G: Operated turbine rotor code  
 P: Non-operated turbine rotor code  
 Cr: Crom  
 W: Wolfram  
 HV: Vickers Hardness  
 MPa: Mega pascal  
 Hf: Hafnium  
 Ta: Talium  
 Ti: Titanium  
 EDS: Energy Dispersive X-Ray Analysis  
 SEM: Scanning Electron Microscope  
 MC: Metal Carbide

#### DECLARATION OF ETHICAL STANDARDS

The author(s) of this article declare that the materials and methods used in this study do not require ethical committee permission and/or legal-special permission.

#### AUTHORS' CONTRIBUTIONS

**Elif UZUN KART:** Analyse with editing the results and wrote the manuscript in English.

**Cemre ÖZGÜL:** Performed the experiments and analyse the results and wrote the manuscript in Turkish.

#### CONFLICT OF INTEREST

There is no conflict of interest in this study.

#### REFERENCES

- [1] Basak, A., Das, S. "Carbide formation in nickel-base superalloy MAR-M247 processed through scanning laser epitaxy (SLE)," *An Addit. Manuf. Conf. SFF*, 460–468, (2016).
- [2] Handa, S. "Precipitation of Carbides in a Super-alloy," *Masters Degree Proj.*, University: 1–33, (2014).
- [3] Goodfellow, A., "Gamma Prime Precipitate Evolution During Aging of a Model Ni-based Super-alloy," *Metall. Mater. Trans. A Phys. Metall. Mater. Sci.*, 49: 3, 718–728, (2018).
- [4] Singh, A., "Mechanisms related to different generations of  $\gamma'$  precipitation during continuous cooling of a nickel base super-alloy," *Acta Mater.*, 61:1, 280–293, (2013).
- [5] Mouritz, P., "*Introduction to Aerospace Materials*", 1st ed. Woodhead Publishing Limited, (2012).
- [6] Liu, L., Zhang, J., and Ai, C., "*Ni-based Super-alloys*," *Encycl. Mater. Met. Alloys*, 294–304, (2022).
- [7] R. Baldan et al., "Solutioning and aging of MAR-M247 Ni-based super-alloy," *J. Mater. Eng. Perform.*, 22: 9, 2574–2579, (2013).
- [8] M. Kvapilova, J. Dvorak, P. Kral, K. Hrbacek, and V. Sklenicka, "Creep behaviour and life assessment of a cast

- nickel - Base super-alloy MAR - M247,” *High Temp. Mater. Process.*, 38: 1, 590–600, (2019).
- [9] Harris, R., Erickson, G.L., “MAR M 247 derivations—CM 247 LC DS alloy, CMSX single crystal alloys, properties and performance,” in *Int. Symp on Super-alloys*, 221–230 (2019).
- [10] Šulák I. and Obrtlík, K., “Effect of tensile dwell on high-temperature low-cycle fatigue and fracture behaviour of cast super-alloy MAR-M247,” *Eng. Fract. Mech.*, 185: 92–100, (2017)
- [11] Rahimian, M., Milenkovic, S. and Sabirov, I., “Microstructure and hardness evolution in MAR-M247 super-alloy processed by controlled cooling and double heat treatment,” *J. Alloys Compd.*, 550: 339–344, (2013).
- [12] Liu, M., Sheng, G., He H., and Jiao, Y., “Microstructural evolution and mechanical properties of TLP bonded joints of Mar-M247 super-alloys with Ni-Cr-Co-W-Ta-B interlayer,” *J. Mater. Process. Technol.*, 246: 245–251, (2017).
- [13] Milenkovic S., Sabirov, I. and Llorca, J., “Effect of the cooling rate on microstructure and hardness of MAR-M247 super-alloy,” *Mater. Lett.*, 73: 216–219, (2012).
- [14] Davis, J. R., “*ASM Speciality Handbook, Nickel Cobalt & Their Alloys*”, 1st ed. ASM International, (2000).
- [15] Harris, K., “Vacuum Induction Refining MM-0011 Mar-M-247 for High Intensity Turbine Rotating Parts,” in *AVS 6th Int’l. Vacuum Metallurgical Conf.*, 7–8, (1979).
- [16] Geddes, X., Leon, H., “*Super-alloys: Alloying and Performance*”, 1st ed. ASM International, (2010).
- [17] Kattus, J., “*Aerospace Structural Metals Handbook, Purdue Research Foundation*”, (1999).
- [18] Szczotok, A. and Rodak, K. “Microstructural studies of carbides in MAR-M247 Ni-based super-alloy,” *IOP Conf. Ser. Mater. Sci. Eng.*, 35:1, (2012).
- [19] Donachie, S., “*Super-alloys: A Technical Guide*”, 2nd ed. ASM International, (2002).
- [20] Martinsson, Å. “Ageing Influence on Ni-based Super-alloys at Intermediate Temperatures (400 – 600°C),” *Luleå Univ. Technol.*, 103, (2006).
- [21] Wawro, W., “MC carbide structures in Mar-M247”, *NASA Contractor Report*, 167892, (1982).
- [22] Bor, Y., Wei, N., Jeng, R and Ko, Y. “Elucidating the effects of solution and double ageing treatment on the mechanical properties and toughness of MAR-M247 super-alloy at high temperature,” *Mater. Chem. Phys.*, 109: 2–3, 334–341, (2008).
- [23] Sims, W., Stoloff, S., “*Super-alloys II, First*” John Wiley & Sons Inc, (1987).
- [24] Durand-Charre, M., “*The Microstructure of Super-alloys*”, Gordon and Breach Science Publishers, (1997).
- [25] Erickson, G., “*ASM Handbook Vol 1, Properties and Selection Iron, Steels, and High Performance Alloys, Specialty Steels and Heat-Resistant Alloys*”, 10th ed. ASM International, (1990).
- [26] Akar, N., Garip Çelik, F. D. "Santrifüj Hassas Döküm Yöntemiyle Üretilen Co-Cr-Mo Süperalaşım Dental Blokların Mikroyapı ve Mekanik Özellikleri Üzerine Atmosfer ve Karbon Miktarının Etkisi". *Politeknik Dergisi*, 1:1, (2021).
- [27] Aytaç, Z., Yücel, N. "Development of a Design Methodology for a Centrifugal Compressor with the Utilization of CFD". *Politeknik Dergisi*, 23:231-239, (2020)